Eur Biophys J (2009) 38:175–184
DOI 10.1007/s00249-008-0365-1

ORIGINAL PAPER

# Analysis of the source of heterogeneity in the osmotic response of plant membrane vesicles

**Karina Alleva · Osvaldo Chara · Moira R. Sutka · Gabriela Amodeo**

Received: 31 March 2008 / Revised: 1 August 2008 / Accepted: 4 August 2008 / Published online: 4 September 2008
© European Biophysical Societies' Association 2008

**Abstract** Plasma membrane vesicles have been widely employed to understand the biophysics of water movements, especially when active aquaporins are present. In general, water permeability coefficients in these preparations outcome from the analysis of the osmotic response of the vesicles by means of light scattering. As from now, this is possible by following a theoretical approach that assumes that scattered light follows a single exponential function and that this behavior is the consequence of vesicle volume changes due to an osmotic challenge. However, some experimental data do not necessarily fit to single exponentials but to double ones. It is argued that the observed double exponential behavior has two possible causes: different vesicle population in terms of permeability or in terms of size distribution. As classical models cannot identify this source of heterogeneity, a mathematical modeling approach was developed based on phenomenological equations of water transport. In the three comparative models presented here, it was assumed that water moves according to an osmotic mechanism across the vesicles, and there is no solute movement across them. Interestingly, when tested in a well described plasma membrane vesicle preparation, the application of these models indicates that the source of heterogeneity in the osmotic response is vesicles having different permeability, clearly discarding the variable size effect. In conclusion, the mathematical approach presented here allows to identify the source of heterogeneity; this information being of particular interest, especially when studying gating mechanisms triggered in water channel activity.

**Keywords** Aquaporins · Stopped flow · Osmotic permeability · Mathematical modeling · Simulations · Water transport

K. Alleva · M. R. Sutka · G. Amodeo (✉)
Laboratorio de Biomembranas,
Departamento de Fisiología y Biofísica,
Facultad de Medicina, Universidad de Buenos Aires,
Paraguay 2155 Piso 7 (C1121ABG), Buenos Aires, Argentina
e-mail: amodeo@dna.uba.ar

O. Chara
Instituto de Física de Líquidos y Sistemas Biológicos, Centro Científico Tecnológico La Plata del Consejo Nacional de Ciencia y Tecnología, Universidad Nacional de La Plata, Comisión de Investigaciones Científicas de la Provincia de Buenos Aires, La Plata, Argentina

O. Chara
Departamento de Fisiología y Biofísica, Facultad de Medicina, Universidad de Buenos Aires, Buenos Aires, Argentina

## Introduction

Aquaporins are ubiquitous transmembrane proteins that specifically control water transport across cell membranes in all living organisms. Their fundamental significance can be highlighted by the following confident facts: (a) certain human genetic diseases and/or physiological conditions can be directly associated to the lack of a particular aquaporin or the presence of mutations in its highly conserved amino acid residues (Agre and Kozono 2003); (b) their participation seems crucial in multifaceted and dissimilar processes such as angiogenesis, cell migration or cell to cell adhesion, therefore opening new perspectives in their physiological and/or pathological function (Harries et al. 2004; Saadoun et al. 2005; Hu and Verkman 2006), (c) their diversity, abundance and complexity in the plant kingdom demands the evaluation of their role in plant growth and development, critical to be considered when

conceiving future crop improvement strategies (Forrest and Bhave 2007).

Unlike ion channels that are easily gauged by electrophysiological techniques, the parameters that have been used to discriminate functional water channels (aquaporins) are restricted to establish: a high osmotic water permeability ($P_f > 0.01$ cm $s^{-1}$), a low Arrhenius activation energy ($E_a < 5$ kcal $mol^{-1}$), inhibition—in some cases—of water transport by mercurials, and a high ratio of osmotic-to-diffusional water permeability coefficients ($P_f/P_d > 1$) (Finkelstein 1987; Verkman et al. 1996).

One of the widely used techniques to determine the water permeability coefficients ($P_f$) is the study of time course of volume changes of isolated membrane vesicles by means of stopped-flow spectrophotometry. As a consequence of an imposed hyperosmotic challenge, the osmotic flow can be followed as the kinetic of scattered light intensity that results from vesicle volume changes.

This technique has largely allowed to characterize membranes with "high water conductance", i.e., high water permeability, being the highest values described: erythrocytes ($P_f \sim 0.02$ cm $s^{-1}$; Raina et al. 1995), plasma membranes of the renal proximal tubule ($P_f \sim 0.01$–$0.04$ cm $s^{-1}$; Meyer and Verkman 1987), type I alveolar epithelial cells ($P_f \sim 0.08$ cm $s^{-1}$; Dobbs et al. 1998) beet root plasma membrane vesicles ($P_f \sim 0.045$ cm $s^{-1}$; Alleva et al. 2006).

One of the key regulatory mechanisms of aquaporins at the protein level is direct gating of the channel (Hedfalk et al. 2006; Verdoucq et al. 2008). As the stopped flow technique allows both monitoring volume flows continuously with time resolution of 2–3 ms and relating osmotic flows to real membrane area without interference of unstirred layers, it also opens new perspectives for evaluating aquaporin gating (Alleva et al. 2006; Hedfalk et al. 2006).

The kinetics of light scattering intensity reflects the time course dependent vesicle volume change when an osmotic challenge is imposed. Usually this kinetics can be interpreted by a single exponential function (Meyer and Verkman 1986; van Heeswijk and van Os 1986). In fact, many membrane vesicles behave in this way, but there are some examples in the literature where kinetics of membrane vesicle volume changes does not fit to single exponentials (van Heeswijk and van Os 1986; Verkman and Masur 1988). For these cases, a double exponential treatment has been proposed. However, the physical reasons of this alternative kinetics are not straightforward, being suggested that the main cause of this fact must be any kind of heterogeneity in the sample. This heterogeneity could be a consequence of two critical aspects: the presence in the sample of vesicles differing in their size or the presence in the sample of vesicles differing in their water permeability. Although any of these situations points to the presence of more than one population of vesicles coexisting in the sample, the available theoretical approaches do not necessarily allow discriminating the source of heterogeneity.

With the purpose of overcoming the limitation of classical data analysis, we have developed a mathematical modeling approach based on the phenomenological differential equations describing osmotic water flow through membranes (Kedem and Katchalsky 1958). This modeling strategy consist of three complement models: one considering one population of vesicles that are homogeneous in their initial size and with only one water pathway (P1_V1 model), other that considers two vesicle populations differing in their initial size but with similar water permeability (P1_V2 model) and the last one assuming two vesicle populations with similar initial sizes but different water permeability (P2_V1 model). This mathematical modeling approach intends to overcome the above-mentioned limitation its goal being to determine the main source of heterogeneity in membrane vesicles samples that do not fit to single exponentials. We present here the application of the proposed model to the analysis of the heterogeneity source in a beet root plasma membrane vesicle preparation having a double exponential kinetics of volume change when exposed to an osmotic challenge.

## Materials and methods

### Isolation of plasma membrane (PM) vesicles

*Beta vulgaris* storage roots (beet roots) plasma membrane vesicles were isolated by aqueous two-phase partitioning, a technique that yields a highly purified preparation with correctly orientated vesicles, i.e., a cytoplasmic side-in orientation (Larsson et al. 1994). The protocol was slightly modified by introducing in the original solutions cation chelators and phosphatase inhibitors to warranty also active aquaporins as described in Gerbeau et al. (2002) and Alleva et al. (2006). Final plasma membrane fraction was centrifuged and then frozen in liquid nitrogen and stored at −70°C. Vesicles used for all the experiments were thawed only once to both minimize damage and warranty functional activity. The PM vesicle enriched fraction contained $9.16 \pm 0.22$ mg protein $ml^{-1}$ ($n = 4$). All procedures were carried at 4°C or on ice. Marker enzymes assays to evaluate the fraction enrichment and/or putative contamination with other membranes and the evaluation of percentage of right-side out vesicles were performed as described elsewhere (Larsson et al. 1994).

### Electron microscopy

PM vesicle enriched fraction was diluted in 100 mM phosphate buffer pH 7.4, centrifuged at 80,000*g* and resuspended with 0.25% (v/v) glutaraldehyde in 100 mM phosphate buffer pH 7.4 for 120 min at 4°C. Samples were washed with this buffer and postfixed for 1 h with 1% (w/v) $OsO_4$ in 100 mM phosphate buffer pH 7.4 at room temperature. Then, the preparation was washed twice with distilled water for 10 min, stained with 5% (w/v) uranyl acetate for 2 h at room temperature, dehydrated in ethanol and embedded in Durcupam. Samples were examined in a microscope at 40,000×.

### Vesicle size

The size of the vesicles was determined with dynamic light scattering (DLS) using a NICOMP 380 particle sizer (PSS-NICOMP Particle Sizing Systems, Santa Barbara, CA). DLS is based on the detection of scattered light at a fixed angle produce by vesicles suspended in a solvent, being the fluctuation of the intensity of scattered light inversely proportional to the diffusion coefficient of the vesicle. The diffusion coefficient then allows the estimation of vesicles radius form Stokes–Einstein equation (Einstein 1905). The instrument is calibrated against latex beads of known diameter distributions, following the instructions of the manufacturer to give the absolute dimensions of the vesicles.

If the vesicles sizes are quite homogeneous, i.e., a unimodal population, its distribution is correctly analyzed by a linear least-squares treatment, but if vesicle size distribution is complex, an analysis based on a nonlinear least-squares treatment of data (based on inversion of the Laplace transform) is applied. NICOMP's manufacturer indicates the cut-off value of Chi-square to treat the sample as a unimodal or bimodal population. Measurements of vesicle size were carried out in membranes that have been submitted to the same dilution protocol as those used in stopped-flow measurements.

### Measurement of the water permeability coefficient by means of stopped-flow light scattering

Kinetics of vesicle volume was followed by 90° light scattering at 500 nm in an Applied Photophysics stopped-flow spectrophotometer (Applied Photophysics, UK), essentially as described previously (Alleva et al. 2006). A transient opening of vesicles allowing re-equilibration of their interior was induced with a 100-fold dilution into an equilibration buffer (50 mM mannitol, 50 mM NaF, 10 mM Tris-Mes, pH 8.3). Water transport was assayed by mixing the equilibrated vesicles with the same volume of a hyperosmotic mannitol media (500 mM mannitol, 50 mM NaF, 10 mM Tris-Mes, pH 8.3), resulting in an inwardly hyperosmotic gradient of approximately 400 mOsm. In each experiment, data from 10 to 12 time course traces were averaged. Replicates were used from a single experiment and then repeated for four different preparations. All measurements were performed at room temperature (23°C).

### Inhibition of water transport

Vesicle shrinking assays of beet root plasma membranes have proven that plant plasma membrane aquaporins (PIPs) at neutral or basic pH have a high water conductance that can be shut down at low pH (Alleva et al. 2006). This assay was therefore employed to dramatically decrease osmotic water permeability. To perform these experiments, buffer solution was adjusted to 10 mM Mes-Tris pH 5.6, therefore acidifying both sides of the vesicle membrane. In each run, PM vesicles were equilibrated with the desired osmotic buffer (low pH, i.e., 5.6 or control pH, i.e., 8.3), then mixed in the stopped-flow chamber with an equal amount of the hyperosmotic mannitol solution at the same pH.

### Simulations procedure

Simulations were performed using Euler method with a custom made software developed in Visual Basic code using an integration step of 0.005 s. This step warranties the order of accuracy and the stability of the Euler method. The procedure results in a prediction of the time course of vesicle relative volume changes following the hypertonic challenge. The software allows model-dependent fitting over the experimental results, to obtain the best-fitted parameters values as well as the simulated and experimental data visualization. Software and source code are available.

### Data analysis and statistics

Akaike Information Criterion (AIC) was used to compare the different models (Akaike 1973). Model with lower *AIC* value was chosen. AIC was calculated as:

$$\mathrm{AIC} = n \ln(\mathrm{SC}) + 2p \quad (1)$$

where, $n$ is the number of experimental data, SC is the residual squares sum and $p$ is the number of parameters. Student's $t$ test was used to analyze significant differences.

## Results

### Measurement of plasma membrane vesicles dimensions

An enriched fraction of PM vesicles from the root parenchyma of beet root was obtained by a two-phase partition

system (Fig. 1). Volume measurements of beet root PM vesicles dimensions were performed by DLS. The technique allows characterizing the size distribution of vesicles by directly analyzing samples exposed to the same experimental conditions that were employed to measure water permeability. Moreover, sampling (number of measured vesicles) is much higher and software processing allows a more sophisticated approach for revealing and unmasking bimodal populations.

Both linear least-square and nonlinear least-square fittings were performed to analyze DLS results (see Sect. "Materials and methods"). Linear-square fitting drove to the subsequent vesicle diameter values 420 ± 33 nm (±SE, $n = 8$). On the other hand, nonlinear least-squares fitting showed a bimodal distribution with the following maximums of vesicle diameter, 225 ± 25 nm and 686 ± 72 nm, (±SE, $n = 8$), being this distribution more probable for vesicle dimensions than unimodal since Chi squared value. Interestingly, the average between the two population diameters obtained by nonlinear least-square distribution analysis (456 ± 48 nm; ±SE, $n = 8$) is not significantly different from the result obtained by linear least-square procedure ($p < 0.05$).

## Osmotic behavior of beet root plasma membrane vesicles

The osmotic permeability of beet root PM vesicles has been previously studied by means of the stopped-flow technique under an osmotic challenge (Alleva et al. 2006). The ideal osmotic behavior of the PM vesicles was confirmed by the observations that: (a) no time dependent change in the light signal was observed after exposure of the vesicles to an iso-osmotic medium and (b) the amplitude of change in light scattering increased with the size of the imposed osmotic gradient and was proportional to the ratio of initial osmolarities (Alleva et al. 2006).

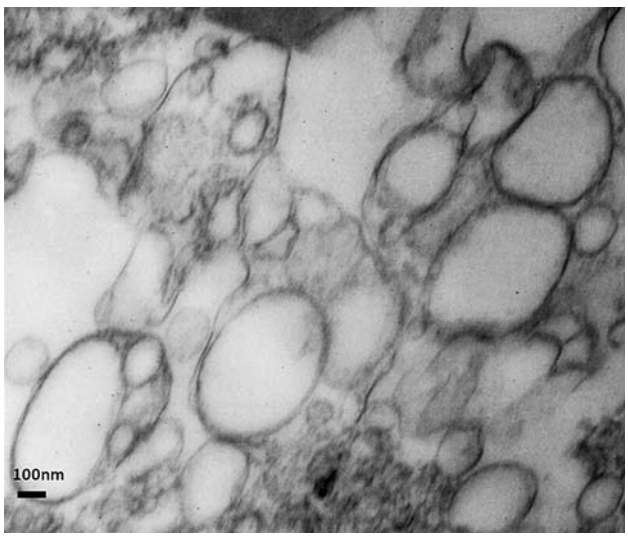


**Fig. 1** Electron micrographs of beet root PM vesicles. The micrograph shows a typical sample. Augmentation used ×40,000

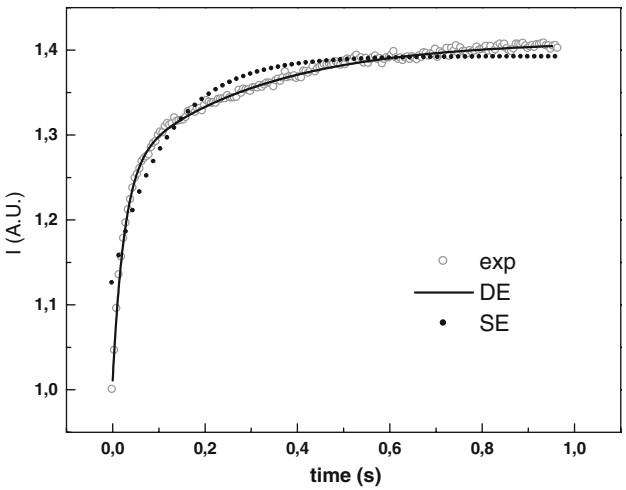


**Fig. 2** PM vesicles time course of scattered light intensity. Representative time course of water efflux in beet root PM vesicles followed by intensity ($I$) of scattered light (arbitrary units, A.U., *open circles*). Fitting to single (*dot line*) and double (*continuous line*) exponentials are shown

Vesicle volume changes followed by light scattered intensity are shown in Fig. 2. According to Akaike criterion, double exponential fitting is more appropriate than single exponential one, revealing some kind of heterogeneity in the sample.

## Mathematical modeling of water transport across plasma membrane vesicles

Three models were proposed based on phenomenological equations of water transport (Kedem and Katchalsky 1958): (i) P1_V1 model, assuming one vesicle population having the same initial volume and only one water permeability, (ii) P2_V1 model, postulating two populations having not necessarily equal water permeability but sharing the same initial volume, and (iii) P1_V2 model, assuming two vesicle populations having different initial volume but only one water permeability. The three models are schemed in Fig. 3.

The following assumptions were considered:

(a) There is no solute movement across the membrane.
(b) The membrane area involved in the water flux varies according to the vesicle volume.
(c) Water is transported by an osmotic mechanism, being the time course of the relative volume change $V_r^j(t)$of population $j$ equal to:

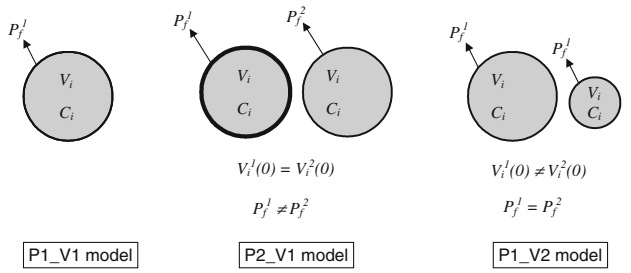


**Fig. 3** Schematic representation of the mathematical models used. In the scheme, vesicles are represented by *grey circles*, being their comparative volumes explicitly shown by the size of these circles. Water permeability coefficients, $P_f$, are represented by the width of the circle limit. P1_V1 model considers only one $P_f$ responsible for water transport and vesicles with the same initial volume. P2_V1 model assumes two vesicle populations with similar initial volume but different $P_f$. P1_V2 model considers two vesicle populations differing in their initial volume but with similar $P_f$

$$\frac{dV_r^j}{dt} = S^j(t)P_f^j V_w(C_i^j(t) - C_e(t)) \quad (2)$$

where $S^j(t)$ is the membrane area, $P_f^j$ is the water osmotic permeability of the vesicle membrane of population $j$, $V_w$ is the water molar partial volume, assumed equal to 18 cm mol$^{-1}$, $C_i^j(t)$, the osmolarity inside the vesicle and $C_e(t)$ is the osmolarity outside the vesicle, modeled as a Heavyside function and experimentally measured.

(d) For the one water pathway model (P1_V1 model), there is one vesicle population which satisfies the following relationship between light scattering intensity and volume:

$$I_r^j(t) = -AV_r^j(t) + B \quad (3)$$

where $I_r^j(t)$ is the relative light scattering intensity due to the population $j$, $V_r^j(t)$ is the relative vesicle volume of the population $j$, $A$ and $B$ are fitted parameters. For the two water pathway models (P2_V1 and P1_V2 models) there are two vesicle populations $j = 1$ and $j = 2$. In this case, the following relationship is proposed:

$$I_r(t) = pNI_r^1(t) + (1-p)NI_r^2(t) \quad (4)$$

where $I_r{}^1$(t) and $I_r^2$(t) are the relative light scattering intensity of each population, $p$ is the proportion of $j = 1$ over the two populations ($j = 1$ and $j = 2$) and $N$ is the total number of vesicles. Each intensity can be associated to the whole relative vesicle volume observed by light scattering data as in the P1_V1 model. Thus, in these cases, the following algebraic expression can be obtained for the total intensity:

$$I_r(t) = -AN\left[pV_r^1(t) + (1-p)V_r^2(t)\right] + 1 + AN \quad (5)$$

## Model simulations

We apply the above-mentioned models to our experimental data in order to identify the one that could better explain the permeability characteristics of beet root PM vesicles.

For P1_V1 model, the vesicle initial volume was the diameter obtained by a linear least-squared fitting of DLS data, while $P_f$ was the fitted parameter. For P1_V2 model, the two initial volumes were chosen from the two maximum provided by non-linear least-square analysis from DLS results. On the other hand, the fitted parameters were the relation of vesicles having each initial volume ($p$) and the only one $P_f$ (corresponding to both groups of vesicles). Finally, for P2_V1 model, the initial volume used was the same that the employed for P1_V1 model, but the fitted parameters were two $P_f$ (one for each putative population of vesicles) and $p$ the proportion of vesicles having each $P_f$.

Model simulations were performed and fitting procedures were applied: Fig. 4 shows the best fitting of each model to experimental data and Table 1 shows the numerical results of such fittings.

The Akaike score (AIC) was calculated for each model fitting, and depending on this criterion, P2_V1 model was the one that could better explain the experimental results. Visual comparison among Fig. 4 a, b and c drive to the same conclusion. By means of this model, we can observe that beet root PM vesicle preparation presents two population of vesicles, $j = 1$ with high water permeability ($0.045 \pm 0.005$ cm s$^{-1}$, mean $\pm$ SE, $n = 4$) and $j = 2$ with low water permeability ($0.0037 \pm 0.0005$ cm s$^{-1}$, mean $\pm$ SE, $n = 4$), $j = 1$ being responsible for 63% of the total response. These estimated $P_f$ values are in agreement with the values obtained by applying the classical model proposed by van Heeswijk and van Os (1986), adding up the advantage of having confidence about the existence of two different water pathways in the sample and discarding the possibility of two vesicle populations in terms of their initial volumes.

## Acidic pH effect

In a previous work, we reported that beet root PM vesicles suffered a dramatic reduction in their $P_f$ due to aquaporin inhibition when the osmotic shock was performed under acidic conditions (Alleva et al. 2006). This inhibitory response of plant plasma membrane aquaporins was also reported by others (Gerbeau et al. 2002; Tournaire-Roux et al. 2003). Moreover, a structural mechanism for pH dependence of PIPs gating was proposed based on the X-ray structures of the closed and open conformations of a plant aquaporin (Törnroth-Horsefield et al. 2006).

Given that previous experiments were performed at pH = 8.3, a second set of experiments were done in acidic conditions. Then, vesicle volume changes followed by light scattered intensity at pH = 5.6 are shown in Fig. 5. Although double exponential and simple exponential functions seem to fit correctly to the time course of light scatter intensity (Fig. 5), it is clear that double exponential

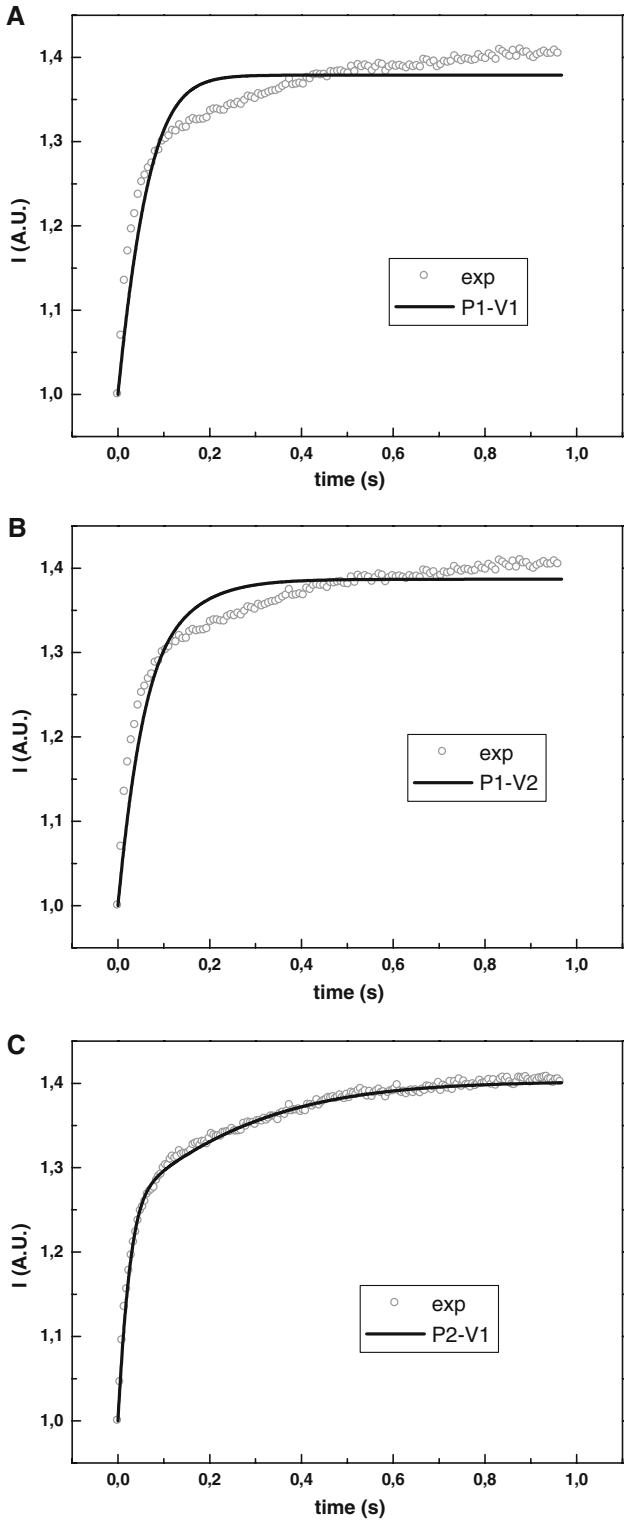


**Fig. 4** Models fitting to experimental data. Fitting of relative volume time course predicted by the three mathematical models (*continuous line*) to experimental data (*open circles*) is shown in each panel. The best fitting was obtained when P2_V1 model was used

**Table 1** Fitted parameters of each mathematical model

| Model | $P_f^1$ (cm s$^{-1}$) | $P_f^2$ (cm s$^{-1}$) | $p$ | *AIC* |
|---|---|---|---|---|
| P2_V1 | 0.045 ± 0.005 | 0.0037 ± 0.0005 | 0.63 ± 0.05 | −10087 |
| P1_V2 | 0.011 ± 0.003 | – | 0.61 ± 0.02 | −5122 |
| P1_V1 | 0.013 ± 0.001 | – | – | −4239 |

The fitted parameters were $P_f^1$ and $P_f^2$, which designates the permeability coefficients of PM vesicle population $j = 1$ and $j = 2$, respectively, and $p$, the proportion of vesicles from population $j = 1$ over total ($j = 1 + j = 2$). Models that considers only one vesicle population in terms of water permeability only have one $P_f$ fitted ($P_f^1$)

function gives a better fit for initial times (Fig. 5, inset). In fact, Akaike criterion shows that double exponential fitting is more correct than single exponential one, revealing again some kind of heterogeneity in the sample. Then, we analyzed by P2_V1 model the light scattering signal versus time of beet root PM vesicles when submitted to an acidic condition under an osmotic challenge. Figures 6 and 7 show that vesicle population with high water permeability, $j = 1$, dramatically reduces its $P_f$ under pH 5.6, this reduction being 98% from its initial value, while the reduction observed in vesicle population with low water permeability, $j = 2$, was not significantly modified ($t$ Student test, $p < 0.05$). Interestingly, the $p$ parameter, which represents the proportion of $j = 1$ over the two populations ($j = 1$ and $j = 2$), was 63%, identical to the one obtained for control pH (8.3).

## Discussion

Mathematical models have undoubtedly extended their application to different fields, including biology (Hernandez 2007; Pafundo et al. 2007) and medicine (Smye and Clayton 2002; Cattoni and Chara 2008). In this work, we proposed this approach as a tool to study the biophysics of water transport, in particular, when membrane vesicles are examined by means of stopped flow spectrophotometry.

As from now, when this technique is employed, the theoretical approximations for calculating $P_f$ assume that light scattering changes after submitting the membrane vesicle preparation to an osmotic shock follows a single exponential function. Starting from phenomenological equations of water transport and equations for physics of light scattering, van Heeswijk and van Os have demonstrated that vesicle light scattered intensity can follow a single exponential kinetics under certain circumstances (van Heeswijk and van Os 1986). This theoretical demonstration simplifies many terms while resolving the differential equations pursuing the single exponential

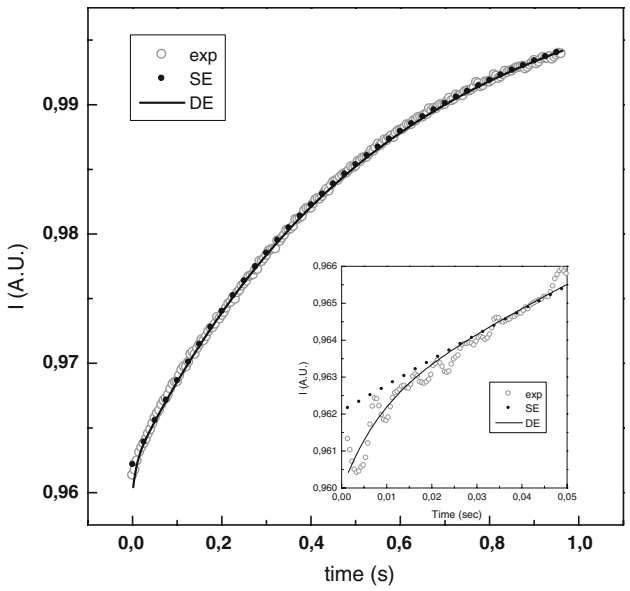


**Fig. 5** PM vesicles time course of light scattered intensity under acidic conditions**.** Time course of water efflux at pH 5.6 in beet root PM vesicles was followed by intensity (*I*) of scattered light (arbitrary units, A.U., *open circles*). Fitting to single (*dot line*) and double (*continuous line*) exponentials are shown. *Inset* details of the first milliseconds of volume change time course showing that the main difference in fitting quality is achieved in this time fraction

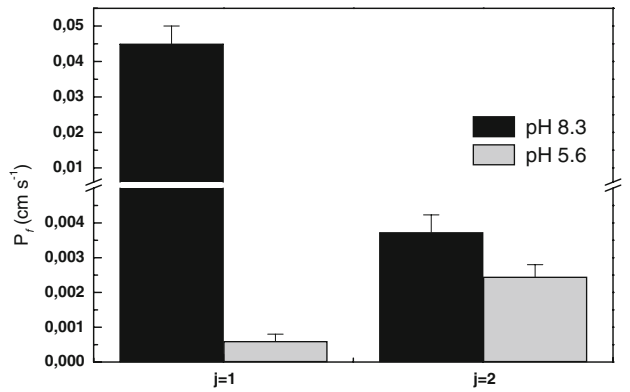


**Fig. 6** Acidic pH effects over PM vesicle populations. Osmotic water permeability ($P_f$) in PM vesicles was tested at two extreme pHs (8.3 and 5.6). P2_V1 model was applied to experimental results at both pHs. For pH 5.6 there was a complete inhibition of water transport for one of the two vesicle population ($j = 1$), while the second vesicle population ($j = 2$) was insensitive to acidification if compared with control (pH 8.3). The *p* parameter was identical in both pH situations, 63%

solution. Even more, this tactic nicely allows obtaining $P_f$ by using the rate constant directly obtained from single exponential fitting. The drawbacks of this theory appears when experimental data do not fit to single exponential, but fits well to double ones. In the previous years, some of these features were extensively analyzed in the plant field, especially when working with protoplasts. For instance, a numerical solution of a theoretical equation describing transient volume in protoplasts was published, where several models with variable $P_f$ were tested (Moshelion et al. 2004). In contrast to these findings, our proposed models are much simpler involving constant $P_f$. Moreover, since our models fit satisfactorily to the experimental data, one should follow Occam's razor principle, in terms that there is no reason to complicate the models by involving variable $P_f$. A more recent work showed that a single exponential approach is also not reasonable to fit the experimental time course of volume changes in protoplasts (Sommer et al. 2007). The authors showed that a model involving the contribution of non-osmotic volume can fit the results. However, this assumption remains inapplicable to model the time course of volume changes in vesicles.

The mathematical models proposed here are based on the numerical solutions of differential equations for water transport and the fitting of simulated results to experimental data. This procedure not only avoids theoretical simplifications but also can account for the reasons of double exponential kinetics of the vesicle samples.

The acceptability of the selected model was based on:

i. goodness-of-fit

We analyzed our experimental data with three different models: (a) P1_V1, (b) P1_V2, and (c) P2_V1 model. According to AIC, the most suitable model was P2_V1 model. First, this indicates that beet root PM preparations present two vesicle populations in terms of water pathways, one with high water osmotic permeability and other with low water osmotic permeability, the one with high water osmotic permeability being responsible for 63% of the total response. Second, the kinetics of light scattering changes observed cannot be explained by different initial volumes; that is, if considering in the sample two vesicle population in terms of size as could be expected when analyzing the DLS information through a nonlinear least square method, still P1_V2 model was inadequate in comparison with P2_V1 model. These results allowed disclosing the source of heterogeneity in the osmotic response of beet root PM vesicles since demonstrate that no matter the initial volumes, a single water pathway (P1_V2 model) resulted inappropriate or poor to explain the double exponential behavior. This reflects that the source of double exponential could hardly be a matter of variable initial volume among the vesicles but is a matter of different permeabilities. Interestingly, this double-exponential behavior was not only reported for membrane vesicles, but also there are some proteoliposomes containing aquaporins that presents a similar performance (e.g., Carbrey et al. 2003; Kozono et al. 2003, Liu et al. 2006). In one of these works, the authors assume that the first constant represents aquaporin transport (i.e., AQP9) and the second one, background

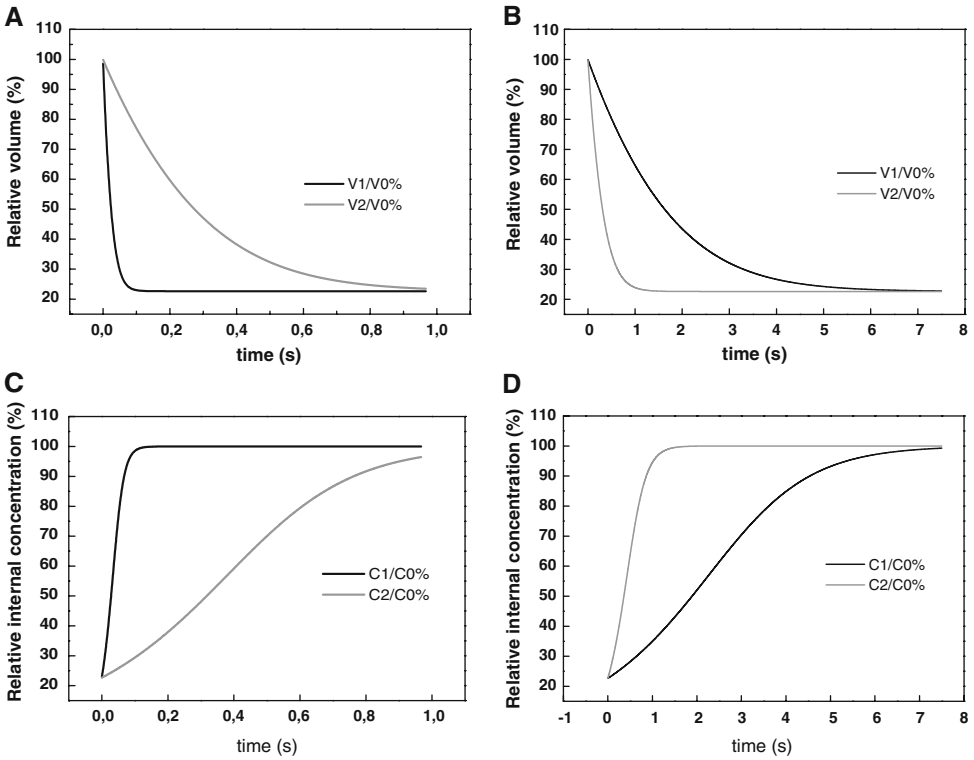


**Fig. 7** Simulation of time course of relative volumes and internal osmolality of PM vesicle populations. (**a**) and (**b**) are the simulated volume changes of PM vesicles for control pH (8.3) and acidic pH (5.6), respectively. It can be seen that in the P2_V1 model each vesicle population for the two pH conditions reaches the expected volume to the equilibrium. The relative volume is $V^1/V_0$ or $V^2/V_0$ where $V^1$ or $V^2$ is the vesicle volume for $j = 1$ or $j = 2$, respectively and $V_0$ is the initial vesicle volume. (**c**) and (**d**) are the simulated relative internal osmolality changes that follow volume changes for control pH (8.3) and acidic pH (5.6), respectively. The P2_V1 model predicts that both vesicle populations can equal the internal osmolality to the external one. The relative osmolarities are $C^1/C_0$ and $C^2/C_0$ where $C^1$ and $C^2$ are the internal osmolality for $j = 1$ and $j = 2$, respectively, being $C_0$ the external osmolality

permeability (Carbrey et al. 2003). Even though the authors do not support this expression with experiments, it is possible that more than one kind of liposomes could be present in the sample: liposomes + aquaporin and liposomes + none/inactive aquaporins. The mathematical models presented here could be an interesting tool to assess the possibility of two liposome populations coexisting in the sample and in estimating the degree of liposomes of each one contributing to the whole volume change response.

ii. accordance of predicted $P_f$ values with $P_f$ calculated by previous models

The two $P_f$ fitted by our P2_V1 model to the experimental data of beet root PM vesicles preparation do not differ from those obtained by fitting the same data to double exponential function and then applying the equation proposed by van Heeswijk and van Os (1986). This means that our mathematical model and previous theoretical considerations completely agree in terms of $P_f$ calculations. Both proposals compensate each other, the advantage of this modeling proposal being its ability to permit a phenomenological interpretation of experimental data allowing the clarification of physics concepts within the mathematical equations. However, on the other hand, its weaker point is the computer-time required for processing, which exceeds the time employed to fit experimental data to exponentials.

iii. prediction of time courses of vesicle volume and osmolality in accordance with the expected ones for the equilibrium

Considering all the experimental conditions assayed at different pH, the simulation of the time courses of volume and osmolality of each vesicle population after the hyperosmotic challenge gives volumes for each population, $j = 1$ and $j = 2$, that converge to 23% of the corresponding initial values, both at low and control pH (Fig. 6a, b). These percentages of reduction in volume are the expected ones for the equilibrium. Moreover, the relative osmolality of PM vesicle populations, $j = 1$ and $j = 2$, reach the equilibrium value (100%, final internal vs. external osmolality) for both pH situations: control and acid pH (Fig. 6c, d). As expected, populations characterized by low

permeability (pH 5.6) reach the equilibrium more slowly, i.e., the time required to reach the equilibrium is longer (close aquaporins) than the observed at control pH (fully open aquaporins).

Taking into account the three above-mentioned statements, we can conclude that the modeling approach presented here is useful to clarify the source of heterogeneity in the osmotic behavior of membrane vesicles following double exponential kinetics.

This approach can be particularly useful to disclose the source of water permeability changes as a consequence of channel activity. Aquaporin regulatory mechanisms open challenges that needs to be completely unveiled, for instance:

(a) Analyzing aquaporin rate of insertion to a membrane, i.e., when the membrane domain is rate-limiting for transcellular water transport and this domain becomes more permeable to water when membranes are exposed to an agonist. This issue was nicely demonstrated in canalicular membrane vesicles (CMV) isolated from rat hepatocytes (Marinelli et al. 2003). The authors observed that CMV fit well to a single-exponential function, showing $P_f$ compatible to low water channel activity, but with 30% inhibitory response to an AQP blocker, dimethyl sulfoxide. Moreover, when CMV were isolated from hepatocytes treated with dibutyryl cAMP, a double-exponential fit was needed, implying two functionally different vesicle populations; one population had $P_f$ values similar to those of CMV from untreated hepatocytes, but the other population had a very high $P_f$.

(b) Analyzing channel gating, i.e., when membrane domains show highly active aquaporins that can be shut down. Based on the X-ray structures of the closed and open conformations of a plant aquaporin (SoPIP2;1), a structural mechanism for PIP gating was proposed considering pH, serine phosphorylation and $Ca^{2+}$ as modulators of channel activity (Hedfalk et al. 2006). It is postulated that transmembrane water channel gating can follow two alternatives models: 'capping' (which caps the channel in the closed state but is displaced to open the pore) and 'pinching' (relying on smaller movements of a single or few residues, which pinch in upon the ar/R constriction region and consequently restricting the passage of water). In a previous work, we demonstrated that PIPs are inhibited by separately increasing cytoplasmic $Ca^{2+}$ and lowering cytoplasmic pH (Alleva et al. 2006).

Here, we show that besides analyzing more complex PM vesicle preparations that initially could not fit to single exponentials, still the shift in $P_f$ could be completely attributed to a shift in water membrane permeability. Moreover, it can be analyzed in detail the populations percentages involved in each component (fast and slow). This was clearly verified when analyzing the permeability of the two water pathways present in beet root PM vesicles under acidic conditions by applying P2_V1 model to experimental results. In this acidic condition, the high water permeability pathway was reduced to a 2% of its initial value, while the low water permeability pathway did not suffer any significant reduction. It is well known that plant plasma membrane aquaporins are shut down by acidic pH, so the result obtained here could be indicating that in beet root PM vesicles are coexisting two differently regulated water pathways, one sensitive to acidic pH and the second with aquaporins that are showing low $P_f$ values (PIP1 subtype?) or are inactive in the experimental conditions and therefore do not show the pH response considerably important.

Therefore, when membrane vesicles under osmotic shock fit double exponential function, the source of heterogeneity can be explained satisfactorily using a mathematical modeling approach as the here presented. This information turns particularly valuable, especially for unraveling water channel activity mechanisms.

**Acknowledgments** The authors deeply thank Dr Steve D. Tyerman for the NICOMP 380 particle sizer for DLS at Adelaide University, Australia and Dr Rolando Rossi for the stopped flow facilities at IQUIFIB FFyB UBA CONICET. OC, MS and GA are career researchers from CONICET. This work was supported by the CONICET (PIP 5154), Universidad de Buenos Aires (UBACyT0407) and ANPCyT (FONCYT PICT04 #15-949), all grants to G.A.

## References

Agre P, Kozono D (2003) Aquaporin water channels: molecular mechanisms for human diseases. FEBS Lett 555:72–78. doi:10.1016/S0014-5793(03)01083-4

Akaike H (1973) A new look at the statistical model identification. IEEE Trans Automat Contr 19:716–723. doi:10.1109/TAC.1974.1100705

Alleva K, Niemietz CM, Sutka M, Maurel C, Parisi M, Tyerman SD et al (2006) Plasma membrane of *Beta vulgaris* storage root shows high water channel activity regulated by cytoplasmic pH and a dual range of calcium concentrations. J Exp Bot 57:609–621. doi:10.1093/jxb/erj046

Carbrey JM, Gorelick-Feldman DA, Kozono D, Praetorius J, Nielsen S, Agre P (2003) Aquaglyceroporin AQP9: solute permeation and metabolic control of expression in liver. Proc Natl Acad Sci USA 100(5):2945–2950. doi:10.1073/pnas.0437994100

Cattoni DI, Chara O (2008) Vacuum effects over the closing of *Enterocutaneous fistulae*: a mathematical modeling approach. Bull Math Biol 70(1):281–296. doi:10.1007/s11538-007-9258-1

Dobbs LG, Gonzalez R, Matthay MA, Carter EP, Allen L, Verkman AS (1998) Highly water-permeable type I alveolar epithelial cells confer high water permeability between the airspace and vasculature in rat lung. Proc Natl Acad Sci USA 95:2991–2996. doi:10.1073/pnas.95.6.2991

Einstein A (1905) Uber die von der molekularkinetischen Theorie der wärme geforderte Bewegung von in ruhenden Flüssigkeiten suspendierten Teilchen. Ann Phys 17:549. doi:10.1002/andp.19053220806

Finkelstein A (1987) Water movement through lipid bilayers, pores, and plasma membranes: theory and reality. Wiley & Sons, New York

Forrest KL, Bhave M (2007) Major intrinsic proteins (MIPs) in plants: a complex gene family with major impacts on plant phenotype. Funct Integr Genomics 4:263–289. doi:10.1007/s10142-007-0049-4

Gerbeau P, Amodeo G, Henzler T, Santoni V, Ripoche P, Maurel C (2002) The water permeability of *Arabidopsis* plasma membrane is regulated by divalent cations and pH. Plant J 1:71–81. doi:10.1046/j.1365-313X.2002.01268.x

Harries WEC, Akhavan D, Miercke LJW, Khademi S, Stroud RM (2004) The channel architecture of aquaporin 0 at a 2.2-Å resolution. Proc Natl Acad Sci USA 101:14045–14050. doi:10.1073/pnas.0405274101

Hedfalk K, Törnroth-Horsefield S, Nyblom M, Johanson U, Kjellbom P, Neutze R (2006) Aquaporin gating. Curr Opin Struct Biol 16:447–456. doi:10.1016/j.sbi.2006.06.009

Hernandez JA (2007) A general model for the dynamics of the cell volume. Bull Math Biol 69:1631–1648. doi:10.1007/s11538-006-9183-8

Hu J, Verkman AS (2006) Increased migration and metastatic potential of tumor cells expressing aquaporin water channels. FASEB J 20:1892–1894. doi:10.1096/fj.06-5930fje

Kedem O, Katchalsky A (1958) Thermodynamic analysis of the permeability of biological membranes to non-electrolytes. Biochim Biophys Acta 27:229–246. doi:10.1016/0006-3002(58)90330-5

Kozono D, Ding X, Iwasaki I, Meng X, Kamagata Y, Agre P et al. (2003) Functional expression and characterization of an archaeal aquaporin. AqpM from *Methanothermobacter marburgensis*. J Biol Chem 278(12):10649–10656. doi:10.1074/jbc.M212418200

Larsson C, Sommarin M, Widell S (1994) Isolation of highly purified plant plasma membranes and separation of inside-out and right-side-out vesicles. Methods Enzymol 228:451–469. doi:10.1016/0076-6879(94)28046-0

Liu K, Nagase H, Huang CG, Calamita G, Agre P (2006) Purification and functional characterization of aquaporin-8. Biol Cell 98(3):153–161. doi:10.1042/BC20050026

Marinelli R, Tietz PS, Caride AJ, Huang BQ, LaRusso NF (2003) Water transporting properties of hepatocyte basolateral and canalicular plasma membrane domains. J Biol Chem 278:43157–43162. doi:10.1074/jbc.M305899200

Meyer MM, Verkman AS (1986) Human platelet osmotic water and nonelectrolyte transport. Am J Physiol 251:C549–C557

Meyer MM, Verkman AS (1987) Evidence for water channels in renal proximal tubule cell membranes. J Membr Biol 96:107–119. doi:10.1007/BF01869237

Moshelion M, Moran N, Chaumont F (2004) Dynamic changes in the osmotic water permeability of protoplast plasma membrane. Plant Physiol 135:2301–2317. doi:10.1104/pp.104.043000

Pafundo DE, Chara O, Faillace MP, Krumschnabel G, Schwarzbaum PJ (2007) Kinetics of ATP release and cell volume regulation of hyposmotically challenged goldfish hepatocytes. Am J Physiol Regul Integr Comp Physiol 294:R220–R233. doi:10.1152/ajpregu.00522.2007

Raina S, Preston GM, Guggino WB, Agre P (1995) Molecular cloning and characterization of an aquaporin cDNA from salivary, lacrimal, and respiratory tissues. J Biol Chem 270:1908–1912. doi:10.1074/jbc.270.4.1908

Saadoun S, Papadopoulos MC, Hara-Chikuma M, Verkman AS (2005) Impairment of angiogenesis and cell migration by targeted aquaporin-1 gene disruption. Nature 434:786–792. doi:10.1038/nature03460

Smye SW, Clayton RH (2002) Mathematical modeling for the new millennium: medicine by numbers. Med Eng Phys 24:565–574. doi:10.1016/S1350-4533(02)00049-8

Sommer A, Mahlknecht G, Obermeyer G (2007) Measuring the osmotic water permeability of the plant protoplast plasma membrane: implication of the non-osmotic volume. J Membr Biol 215:111–123. doi:10.1007/s00232-007-9011-6

Törnroth-Horsefield S, Wang Y, Hedfalk K, Johanson U, Karlsson M, Tajkhorshid E et al (2006) Structural mechanism of plant aquaporin gating. Nature 439:688–694. doi:10.1038/nature04316

Tournaire-Roux C, Sutka M, Javot H, Gout E, Gerbeau P, Luu DT et al (2003) Cytosolic pH regulates root water transport during anoxic stress through gating of aquaporins. Nature 425:393–397. doi:10.1038/nature01853

van Heeswijk MPE, van Os CH (1986) Osmotic water permeabilities of brush border and basolateral membrane vesicles from rat renal cortex and small intestine. J Membr Biol 92:183–193. doi:10.1007/BF01870707

Verdoucq L, Grondin A, Maurel C (2008) Structure-function analysis of plant aquaporin AtPIP2;1 gating by divalent cations and protons. Biochem J (Jul):21. Epub ahead of print.

Verkman AS, Masur SK (1988) Very low osmotic water permeability and membrane fluidity in isolated toad bladder granules. J Membr Biol 104:241–251. doi:10.1007/BF01872326

Verkman AS, Van Hoek AN, Ma T, Frigeri A, Skach WR, Mitra A et al (1996) Water transport across mammalian cell membranes. Am J Physiol 270:C12–C30